$$q = \begin{bmatrix} \cos\dfrac{\phi}{2} & \vec{u}\sin\dfrac{\phi}{2} \end{bmatrix}^T = q_0 + q_1 i + q_2 j + q_3 k = \begin{bmatrix} q_0 \\ \tilde{q} \end{bmatrix} \in Q \tag{1}$$

with q_0, q_1, q_2, and q_3 are real numbers and i, j, and k are the components of the vector $\vec{u}$. Q can be defined as:

$$Q = \left\{ q / q^T q = 1,\ q_0 \in \Re^{1\times 1}, \tilde{q} = \begin{bmatrix} q_1 & q_2 & q_3 \end{bmatrix}^T \in \Re^{3\times 1} \right\} \tag{2}$$

Let us define some quaternion's proprieties that will be used later in the proposed approach. The multiplication of two quaternions $q_a = \begin{bmatrix} q_{a0} & \tilde{q}_a^T \end{bmatrix}^T$ and $q_b = \begin{bmatrix} q_{b0} & \tilde{q}_b^T \end{bmatrix}^T$ is expressed as:

$$q_a \otimes q_b = \begin{bmatrix} q_{a0} & -\tilde{q}_a^T \\ \tilde{q}_a & I_{3\times 3} q_{a0} + \begin{bmatrix} \tilde{q}_a^{\times} \end{bmatrix} \end{bmatrix} \begin{bmatrix} q_{b0} \\ \tilde{q}_b \end{bmatrix} \tag{3}$$

where

$$\begin{bmatrix} \tilde{q}_a^{\times} \end{bmatrix} = \begin{bmatrix} q_{a1} \\ q_{a2} \\ q_{a3} \end{bmatrix}^{\times} = \begin{bmatrix} 0 & -q_{a3} & q_{a2} \\ q_{a3} & 0 & -q_{a1} \\ -q_{a2} & q_{a1} & 0 \end{bmatrix} \tag{4}$$

The unit quaternion satisfies the following constraint:

$$q_0^2 + q_1^2 + q_2^2 + q_3^2 = 1 \tag{5}$$

Using quaternion representation, there are two means to express a vector rotation in space. Let x_q and y_q be two quaternions associated with the vectors $x \in \Re^{3\times 1}$ and $y \in \Re^{3\times 1}$ expressed in N and B, respectively:

$$\begin{cases} x_q = \begin{bmatrix} 0 & x^T \end{bmatrix}^T \\ y_q = \begin{bmatrix} 0 & y^T \end{bmatrix}^T \end{cases} \tag{6}$$

1) x_q and y_q are bounded by the following relation:

$$x_q = q \otimes y_q \otimes \overline{q} \tag{7}$$

where $\overline{q}$ represents the complementary quaternion that can be expressed as:

$$\overline{q} = \begin{bmatrix} q_0 & -\tilde{q}^T \end{bmatrix}^T \tag{8}$$

2) The operation using equation (7) is equivalent to a multiplication by a rotation matrix:

$$x = M_N^B(q)\, y \tag{9}$$

where the rotation matrix $M_N^B(q)$ is expressed in terms of quaternion by the following formula [14]:

$$M_N^B(q) = \left(q_0^2 - \tilde{q}^T\tilde{q}\right) I_{3\times 3} + 2\left(\tilde{q}\tilde{q}^T - q_0\left[\tilde{q}^\times\right]\right) \tag{10}$$

where $\left[\tilde{q}^\times\right]$ is given by (4) with replacing $\tilde{q}_a$ by $\tilde{q}$.
Finally, one obtains:

$$M_N^B(q) = \begin{bmatrix} 2\left(q_0^2+q_1^2\right)-1 & 2\left(q_1q_2+q_0q_3\right) & 2\left(q_1q_3-q_0q_2\right) \\ 2\left(q_1q_2-q_0q_3\right) & 2\left(q_0^2+q_2^2\right)-1 & 2\left(q_0q_1+q_2q_3\right) \\ 2\left(q_0q_2+q_1q_3\right) & 2\left(q_2q_3-q_0q_1\right) & 2\left(q_0^2+q_3^2\right)-1 \end{bmatrix} \tag{11}$$

3.2. Sensor-based framework

The sensors configuration consists of 3-axis gyroscope, 3-axis accelerometer and 3-axis magnetometer containing MEMS technologies. A detailed study of these sensors is given in [15]. Their outputs are expressed in the frame B, respectively, by:

$$\omega_G = \begin{bmatrix} \omega_{Gx} & \omega_{Gy} & \omega_{Gz} \end{bmatrix}^T = \omega + b + \delta_G \tag{12}$$

$$f = \begin{bmatrix} f_x & f_y & f_z \end{bmatrix}^T = M_N^B(q)\left(g + a\right) + \delta_f \tag{13}$$

$$h = \begin{bmatrix} h_x & h_y & h_z \end{bmatrix}^T = M_N^B(q)\, m + \delta_h \tag{14}$$

where $\omega = \begin{bmatrix} \omega_x & \omega_y & \omega_z \end{bmatrix}^T \in \Re^{3\times 1}$ represents the real angular velocity vector measured in B. $g = \begin{bmatrix} 0 & 0 & 9.81 \end{bmatrix}^T \in \Re^{3\times 1}$ and $a = \begin{bmatrix} a_x & a_y & a_z \end{bmatrix}^T \in \Re^{3\times 1}$ represent the gravity vector and the body acceleration, respectively. a and g are expressed in N. $m = \begin{bmatrix} m_x & 0 & m_z \end{bmatrix}^T = \begin{bmatrix} \|m\|\cos(\theta) & 0 & \|m\|\sin(\theta) \end{bmatrix}^T \in \Re^{3\times 1}$ represents the magnetic field measured in N. The theoretical model of the magnetic field nearest to reality considers a magnetic field vector with an inclination angle $\theta = 60°$ and a norm vector $\|m\| = 0.5$ Gauss [16]. $b = \begin{bmatrix} b_x & b_y & b_z \end{bmatrix}^T \in \Re^{3\times 1}$ is a function varying slowly in time

and representing an unknown gyro-bias modeled by a Gauss-Markov process [17]. It is described by:

$$\dot{b} = -T^{-1}b \tag{15}$$

where $T = \tau I_{3\times 3}$ is a diagonal matrix of the time constant τ.

$\delta_G \in \Re^{3\times 1}$, $\delta_f \in \Re^{3\times 1}$ and $\delta_h \in \Re^{3\times 1}$ are assumed uncorrelated white Gaussian measurements noises with null mean and covariance matrix.

Since a normalized unit quaternion is used, then g is also normalized to a unit vector such as:

$$g = \frac{\begin{bmatrix}0 & 0 & 9.81\end{bmatrix}^T}{\sqrt{9.81^2}} = \begin{bmatrix}0 & 0 & 1\end{bmatrix}^T \tag{16}$$

In the same way as for the accelerometer, m is normalized to a unit vector such as:

$$m = \frac{\begin{bmatrix}0.5\cos(60°) & 0 & 0.5\sin(60°)\end{bmatrix}^T}{\sqrt{0.5^2\cos^2(60°)+0.5^2\sin^2(60°)}} = \begin{bmatrix}0.5 & 0 & \sqrt{3}/2\end{bmatrix}^T \tag{17}$$

3.3. Rigid-body kinematic model

The kinematic equation, expressed using the unit quaternion, describes the relation between the variation of the rigid-body attitude in time and the angular velocity. It is given by [14]:

$$\begin{bmatrix}\dot{q}_0 \\ \dot{\tilde{q}}\end{bmatrix} = \frac{1}{2}\begin{bmatrix}-\tilde{q}^T \\ I_3 q_0 + \left[\tilde{q}^\times\right]\end{bmatrix}\omega \tag{18}$$

where $\omega = \begin{bmatrix}\omega_x & \omega_y & \omega_z\end{bmatrix}^T$ represents the real angular velocity rate vector of a rigid-body measured by gyroscope in the frame B. $\left[\tilde{q}^\times\right]$ is given by (4) with replacing $\tilde{q}_a$ by $\tilde{q}$.

4. Design of the complementary nonlinear observer approach for the rigid-body attitude estimation

In this paper, the objective is to design a rigid-body attitude estimation algorithm based on inertial and magnetic MEMS sensors (low-cost and low-power sensors). The proposed approach will be subsequently used to estimate the orientation, under several motions, of the studied animal's specie: the king penguin. Amongst various

navigation systems, strap-down system based on the integral of the angular velocity from gyroscope leads to a good attitude estimates (in dynamic situations) for short time but suffers from gyro-bias which causes the orientation estimates to drift away from the true orientation rapidly. Accelerometer and magnetometer are good sensors in attitude estimation for static and quasi-static motion but with poor dynamic performance [2].

We propose an observer approach to take advantages from accelerometers, magnetometers and gyroscopes in order to estimate the most accurate attitude. Moreover, the proposed solution includes the estimation of rate gyros biases to compensate angular velocity measurements. It important to stress that the resulting approach structure is complementary: high bandwidth rate gyro measurements are combined with low bandwidth vector observations to provide an accurate estimates of the attitude [17]. In our knowledge, the proposed approach using this triad of sensors is the first work applied in Bio-logging area [18].

Firstly, one considers that the real angular velocity vector ω is written as:

$$\omega = \omega_G - b - \delta_G \tag{19}$$

To achieve our goal, let us consider the following nonlinear system described in (20) and obtained from (18), (15) and (19):

$$\begin{cases} \begin{bmatrix} \dot{q} \\ \dot{b} \end{bmatrix} = \begin{bmatrix} \frac{1}{2}\begin{bmatrix} -\tilde{q}^T \\ I_{3\times3}q_0 + [\tilde{q}^\times] \end{bmatrix}\omega \\ -T^{-1}b \end{bmatrix} = \begin{bmatrix} \frac{1}{2}\begin{bmatrix} -q_1 & -q_2 & -q_3 \\ q_0 & -q_3 & q_2 \\ q_3 & q_0 & -q_1 \\ -q_2 & q_1 & q_0 \end{bmatrix}\left[\omega_G - b - \delta_G\right] \\ \begin{bmatrix} -\frac{1}{\tau} & 0 & 0 \\ 0 & -\frac{1}{\tau} & 0 \\ 0 & 0 & -\frac{1}{\tau} \end{bmatrix} b \end{bmatrix} \\ y = q' = \begin{bmatrix} q'_0 & q'_1 & q'_2 & q'_3 \end{bmatrix}^T \end{cases} \tag{20}$$

where $q \in \Re^{4\times1}$ is the quaternion and $b \in \Re^{3\times1}$ is the bias (system's states). $I_{3\times3} \in \Re^{3\times3}$ is an identity matrix. $q' \in \Re^{4\times1}$ is the system output that is determined based on optimal fusion of accelerometer and magnetometer measurements. The method that allows to calculate q' is presented in the next section.

In order to estimate the attitude, the following complementary nonlinear attitude observer is proposed:

$$\begin{cases} \dot{\hat{q}} = \frac{1}{2}\begin{bmatrix} -\hat{\tilde{q}}^T \\ I_{3\times 3}\hat{q}_0 + \left[\hat{\tilde{q}}^{\times}\right] \end{bmatrix}\left[\omega_G - \hat{b} + k_1\tilde{q}_e\right] \\ \dot{\hat{b}} = -T^{-1}\hat{b} - k_2\tilde{q}_e \end{cases} \tag{21}$$

$\hat{q}$ and $\hat{b}$ represent the estimated states. The observer gains $k_1, k_2 \in \Re^{1\times 1}$ are positive constants. $\left[\hat{\tilde{q}}^{\times}\right]$ is given by (4) with replacing $\tilde{q}_a$ by $\hat{\tilde{q}}$. $\tilde{q}_e \in \Re^{3\times 1}$ represents the vector part of the error quaternion q_e.

q_e is obtained by using the quaternion product (3) between the measured quaternion q' and the complementary estimated quaternion $\overline{\hat{q}}$ with replacing q_a by $\overline{\hat{q}}$ and q_b by q':

$$q_e = \overline{\hat{q}} \otimes q' = \begin{bmatrix} q_{e0} & \tilde{q}_e^T \end{bmatrix}^T \tag{22}$$

Based on [2], [19], a detailed mathematical analysis of the observer convergence and the global stability are derived. Suppose that $\delta_G = 0$ and $q' \approx q$.

Theorem 1: Consider the kinematic equation (18) for a time-varying $q(t)$ and with measurements given by q' and ω_G. Let $\left(\hat{q}(t), \hat{b}(t)\right)$ denote the solution of (21). Define error variables $q_e = \overline{\hat{q}} \otimes q'$ and $b_e = b - \hat{b}$. Then, the error $\left[q_e^T(t) \quad b_e^T(t)\right]$ is globally asymptotically stable to $\begin{bmatrix} \pm 1 & 0 & 0 & 0 & 0 & 0 & 0 \end{bmatrix}$. For almost all initial conditions $\left(q_e(t_0), b_e(t_0)\right)$, the trajectory $\left(\hat{q}(t), \hat{b}(t)\right)$ converges to the trajectory $\left(q(t), b\right)$.

Proof: Let us consider the two error equations given by:

$$q_e = \begin{bmatrix} q_{e0} & q_{e1} & q_{e2} & q_{e3} \end{bmatrix}^T = \overline{\hat{q}} \otimes q' \tag{23}$$

$$b_e = \begin{bmatrix} b_{ex} & b_{ey} & b_{ez} \end{bmatrix}^T = b - \hat{b} \tag{24}$$

Suppose that $q' \approx q$ and using the definition of quaternion product $\otimes$ given in (3), equation (23) can be written as:

$$q_e = \begin{bmatrix} q_0\hat{q}_0 + q_1\hat{q}_1 + q_2\hat{q}_2 + q_3\hat{q}_3 \\ -q_0\hat{q}_1 + q_1\hat{q}_0 + q_2\hat{q}_3 - q_3\hat{q}_2 \\ -q_0\hat{q}_2 - q_1\hat{q}_3 + q_2\hat{q}_0 + q_3\hat{q}_1 \\ -q_0\hat{q}_3 + q_1\hat{q}_2 - q_2\hat{q}_1 + q_3\hat{q}_0 \end{bmatrix} \tag{25}$$

Now, differentiating (24) and (25), then one obtains:

$$\begin{cases} \dot{q}_e = \begin{bmatrix} \dot{q}_0\hat{q}_0 + q_0\dot{\hat{q}}_0 + \dot{q}_1\hat{q}_1 + q_1\dot{\hat{q}}_1 + \dot{q}_2\hat{q}_2 + q_2\dot{\hat{q}}_2 + \dot{q}_3\hat{q}_3 + q_3\dot{\hat{q}}_3 \\ -\dot{q}_0\hat{q}_1 - q_0\dot{\hat{q}}_1 + \dot{q}_1\hat{q}_0 + q_1\dot{\hat{q}}_0 + \dot{q}_2\hat{q}_3 + q_2\dot{\hat{q}}_3 - \dot{q}_3\hat{q}_2 - q_3\dot{\hat{q}}_2 \\ -\dot{q}_0\hat{q}_2 - q_0\dot{\hat{q}}_2 - \dot{q}_1\hat{q}_3 - q_1\dot{\hat{q}}_3 + \dot{q}_2\hat{q}_0 + q_2\dot{\hat{q}}_0 + \dot{q}_3\hat{q}_1 + q_3\dot{\hat{q}}_1 \\ -\dot{q}_0\hat{q}_3 - q_0\dot{\hat{q}}_3 + \dot{q}_1\hat{q}_2 + q_1\dot{\hat{q}}_2 - \dot{q}_2\hat{q}_1 - q_2\dot{\hat{q}}_1 + \dot{q}_3\hat{q}_0 + q_3\dot{\hat{q}}_0 \end{bmatrix} \\ \dot{b}_e = \dot{b} - \dot{\hat{b}} \end{cases} \quad (26)$$

Substitute $\dot{q} = \begin{bmatrix} \dot{q}_0 & \dot{q}_1 & \dot{q}_2 & \dot{q}_3 \end{bmatrix}^T$, $\dot{b} = \begin{bmatrix} \dot{b}_x & \dot{b}_y & \dot{b}_z \end{bmatrix}^T$, $\dot{\hat{q}} = \begin{bmatrix} \dot{\hat{q}}_0 & \dot{\hat{q}}_1 & \dot{\hat{q}}_2 & \dot{\hat{q}}_3 \end{bmatrix}^T$ and $\dot{\hat{b}} = \begin{bmatrix} \dot{\hat{b}}_x & \dot{\hat{b}}_y & \dot{\hat{b}}_z \end{bmatrix}^T$ given in (20) and (21).

Finally, the observation error dynamic's is written as follows:

$$\begin{cases} \dot{q}_e = \frac{1}{2}\begin{bmatrix} 0 & \begin{bmatrix} b_e + k_1\tilde{q}_e \end{bmatrix}^T \\ -\begin{bmatrix} b_e + k_1\tilde{q}_e \end{bmatrix} & \begin{bmatrix} 2\omega^{\times} \end{bmatrix} + \begin{bmatrix} \begin{bmatrix} b_e + k_1\tilde{q}_e \end{bmatrix}^{\times} \end{bmatrix} \end{bmatrix} \begin{bmatrix} q_{e0} \\ \tilde{q}_e \end{bmatrix} \\ \dot{b}_e = -T^{-1}b_e + k_2\tilde{q}_e \end{cases} \quad (27)$$

It is easily verified that:

$$\begin{bmatrix} q_e^T & b_e^T \end{bmatrix} = \begin{bmatrix} +1 & 0 & 0 & 0 & 0 & 0 & 0 \end{bmatrix} \quad (28)$$

and

$$\begin{bmatrix} q_e^T & b_e^T \end{bmatrix} = \begin{bmatrix} -1 & 0 & 0 & 0 & 0 & 0 & 0 \end{bmatrix} \quad (29)$$

are the equilibrium states of the error dynamics (27).
Let us consider a domain D as:

$$D = \left\{ q_e \in \Re^{4\times 1} / \ -1 \le q_e(i) \le 1 \text{ , } \{\text{i=1..4}\} \text{ and } b_e \in \Re^{3\times 1} / \ -\infty < b_e(i) < +\infty \text{ , } \{\text{i=1..3}\} \right\} \quad (30)$$

Let us define two candidate Lyapunov functions V_1 and V_2. These functions are continuous, positive definite, bounded and belong to the class C^2 as:

$$V_1 = \frac{1}{2}b_e^T b_e + k_2\left((1 - q_{e0})^2 + \tilde{q}_e^T\tilde{q}_e \right), \quad \text{if } q_{e0} \ge 0 \quad (31)$$

$$V_2 = \frac{1}{2}b_e^T b_e + k_2\left((1 + q_{e0})^2 + \tilde{q}_e^T\tilde{q}_e \right), \quad \text{if } q_{e0} < 0 \quad (32)$$

In our case, the motion can change randomly, and then q_{e0} can take positive or negative value according to the value of ϕ. If we choose the case $q_{e0} \ge 0$, then we consider the Lyapunov function in (31). Equation (31) can be written also as:

$$V = \frac{1}{2} b_e^T b_e + k_2 \left(2\left(1 - q_{e0}\right)\right) \tag{33}$$

When differentiating (33) and using (27), one obtains:

$$\dot{V} = -2k_2 \dot{q}_{e0} + b_e^T \dot{b}_e \tag{34}$$

Finally, one obtains:

$$\dot{V} = -k_2 k_1 \tilde{q}_e^T \tilde{q}_e - b_e^T T^{-1} b_e \tag{35}$$

Since $0 \le q_{e0} \le 1$, then:

$$\tilde{q}_e^T \tilde{q}_e = 1 - q_{e0}^2 \ge 0 \tag{36}$$

When the gains k_1, k_2 are positive constants, we can write:

$$\dot{V} \le 0 \tag{37}$$

It is clear that $\dot{V}$ is negative semi-definite and for equilibrium states (28) and (29), the condition $V\left(q_e, b_e\right) = \dot{V}\left(q_e, b_e\right) = 0$ is satisfied. Thus, $\left(\tilde{q}_e, b_e\right) \to 0$ and consequently $q_{e0} \to \pm 1$ (the norm of q_e is always equal 1 [13]).

In the same way, for the case $q_{e0} < 0$, the associated Lyapunov function (32) leads to the same result given by (35).

Let $\Upsilon = \left\{\left(q_e, b_e\right) \in D / \ \dot{V}\left(q_e, b_e\right) = 0\right\}$. Therefore, the only solution that can stay identically in Υ is the trivial solutions in (28) and (29). Now, applying Krasovskii-LaSalle's principle [20], one can conclude that the equilibrium states (28) and (29) are globally asymptotically stable, which ends the proof.

■

5. Optimal determination of q' from vector observations

In this section, one presents an optimal method to determine the attitude q' that is used as measurements for the nonlinear observer in (21). The problem of optimal attitude determination algorithm using two sensor's measurements (vector observations) is known as the *Wahba's problem* [21]. In this paper, we consider the earth's magnetic field $m = \begin{bmatrix} m_x & m_y & m_z \end{bmatrix}^T$ defined in (17) and the gravity vector $g = \begin{bmatrix} g_x & g_y & g_z \end{bmatrix}^T$ expressed in (16) as vector observations. These quantities are locally constant in the Earth-fixed frame N.

To solve this problem, let us define firstly the modelling error:

$$\delta\left(\hat{q}\right) = \left(y - \hat{y}\right) \tag{38}$$

where y represents the theoretical values of gravity and earth's magnetic fields:

$$y = \begin{bmatrix} g_x & g_y & g_z & m_x & m_y & m_z \end{bmatrix}^T \tag{39}$$

$\hat{y}$ depicts the estimated values of g and m:

$$\hat{y} = \begin{bmatrix} \hat{g}_x & \hat{g}_y & \hat{g}_z & \hat{m}_x & \hat{m}_y & \hat{m}_z \end{bmatrix}^T \tag{40}$$

Note that these estimated values are obtained from the followings two equations:

$$\hat{g}_q = \begin{bmatrix} 0 & \hat{g}_x & \hat{g}_y & \hat{g}_z \end{bmatrix}^T = \hat{q} \otimes f_q \otimes \bar{\hat{q}} \tag{41}$$

$$\hat{m}_q = \begin{bmatrix} 0 & \hat{m}_x & \hat{m}_y & \hat{m}_z \end{bmatrix}^T = \hat{q} \otimes h_q \otimes \bar{\hat{q}} \tag{42}$$

where f_q represents the quaternion form associated to the acceleration vector as $f_q = \begin{bmatrix} 0 & f_x & f_y & f_z \end{bmatrix}^T$ and h_q the quaternion form associated to the earth's magnetic field vector as $h_q = \begin{bmatrix} 0 & h_x & h_y & h_z \end{bmatrix}^T$. $\hat{q}$ depicts the estimated attitude form the nonlinear observer in (21).

To minimize the error $\delta(\hat{q})$, an iterative method is used to locate the minimum of the scalar squared error criterion function:

$$J(\hat{q}) = \delta(\hat{q})^T \delta(\hat{q}) \tag{43}$$

Several approaches have proved to be effective as standard technique for nonlinear least-squares problems. In this paper, Levenberg Marquardt Algorithm (LMA) is used to minimise the nonlinear function $J(\hat{q})$. It outperforms the Gauss-Newton Algorithm (GNA) and the method of gradient descent. The LMA is more robust than GNA in the region of local minimum [22]. Then the unique minimum can be written in the following form [23]:

$$\zeta(\hat{q}) = c\left[H^T H + \lambda I_{3\times 3} \right]^{-1} H^T \delta(\hat{q}) \tag{44}$$

where λ is a constant that adjusts the convergence rate of the algorithm and guarantees that the inverted term will be non-singular. c is a smoothing parameter chosen between 0 and 1 [6].

$H \in \Re^{6\times 3}$ is the Jacobian matrix defined as [24]:

$$H = -2\begin{bmatrix} \begin{bmatrix} \hat{g}^\times \end{bmatrix} & \begin{bmatrix} \hat{m}^\times \end{bmatrix} \end{bmatrix}^T \tag{45}$$

where $\begin{bmatrix} \hat{g}^\times \end{bmatrix}$ and $\begin{bmatrix} \hat{m}^\times \end{bmatrix}$ are defined in (4) with replacing $\tilde{q}_a$ by $\hat{g}$ and $\hat{h}$.

Then, from (45), one obtains the following matrix:

$$H = -2\begin{bmatrix} 0 & -\hat{g}_z & \hat{g}_y & 0 & -\hat{m}_z & \hat{m}_y \\ \hat{g}_z & 0 & -\hat{g}_x & \hat{m}_z & 0 & -\hat{m}_x \\ -\hat{g}_y & \hat{g}_x & 0 & -\hat{m}_y & \hat{m}_x & 0 \end{bmatrix}^T \tag{46}$$

Note that $\zeta(\hat{q}) \in \Re^{3\times 1}$ represents the vector part of the error quaternion of the LMA. Then one takes $\zeta(\hat{q}) = \tilde{q}_{error}$. Finally, to obtain the quaternion q', that is used after in (22), one uses the following equation:

$$q'(k+1) = q'(k) \otimes \begin{bmatrix} 1 & \tilde{q}_{error} \end{bmatrix}^T \tag{47}$$

For $k = [1..n]$ (n is the final integration step), one chooses to use always the condition $q'(k) = \hat{q}(k)$ to obtain faster convergence of the LMA. Note that the scalar part of the error quaternion $\begin{bmatrix} 1 & \tilde{q}_{error} \end{bmatrix}^T$ is very close to unit since the incremental quaternion corresponds to a small angle rotation and then the only dynamics of the system will be contained in the vector part of the perturbation quaternion.
Note that this algorithm is limited to the lowest frequencies of the natural panel of movements [2] (the static or quasi-static situations) and the values of q' are strongly disturbed in dynamic situations. q' is smoothed after by the proposed observer in (21).

6. Simulation results

This section aims at illustrating the performance and accuracy of the complementary nonlinear observer designed in (21). Some numerical simulations were carried out under Matlab to estimate the rigid-body attitude based on the measurable inertial and magnetic measurements. To achieve these simulations, one starts by generating a theoretical example of attitude variation that was the subject of angular velocity data over 100 sec. The kinematic differential equation in (18) is used to obtain the continuous time motion in quaternion representation based on the considered angular velocity measurements. The obtained motion (quaternion term) is used in these simulations as reference and which will be estimated after by the proposed observer. To represent the sensor imperfections, an additive random zero-mean white Gaussian noise was considered for all measurements (see Table 1).

The sampling and calculation rate was chosen as 100Hz for all measurements (0.01sec). The angular velocity measurements are also assumed to be corrupted by a theoretical bias. This latter is generated based on equation (15). Notice that the bias is very common and undesirable characteristic of low-cost rate gyros. The observer gains k_1 and k_2 that guarantee convergent estimates, are set according to the considered sensor noise levels and sampling rate as: $k_1 = 25$ and $k_2 = 40$. The constant c used in the LMA is set to $c = 1/3$. In these simulations, one chooses to initialize the theoretical states of the model (the quaternion q and bias b) and those

of the observer with different random values. These conditions are summarized in Table 2. Notice that this choice allows illustrating the convergence of the observer although it was initialized far from the actual states.

The time history of the seven states to be estimated (quaternion and bias components) and observer estimates are shown in Figs. 3 and 4. Despite the nonlinear observer and the theoretical model of the quaternion and bias were initialized with different initial conditions, one can note that the estimated quaternion and bias converge rapidly towards its theoretical values. Notice that one has tried to change the initial conditions and the same performance was obtained. It is clear that the domain of attraction seems to be large enough since the states are initialized far from their true values and the observer converges quite fast. Notice that the nonlinear observer copes well with the rate gyro bias. Moreover the noises of the accelerometer and magnetometer are rejected. In order to evaluate the overall attitude estimation performance, one chooses to plot the time history evolution of the estimation errors on the quaternion and bias. Figs. 5 and 6 depict the convergence of these errors towards zero during the motion. These obtained results show the effectiveness of the complementary nonlinear observer to the attitude estimation during the considered rigid-body motion.

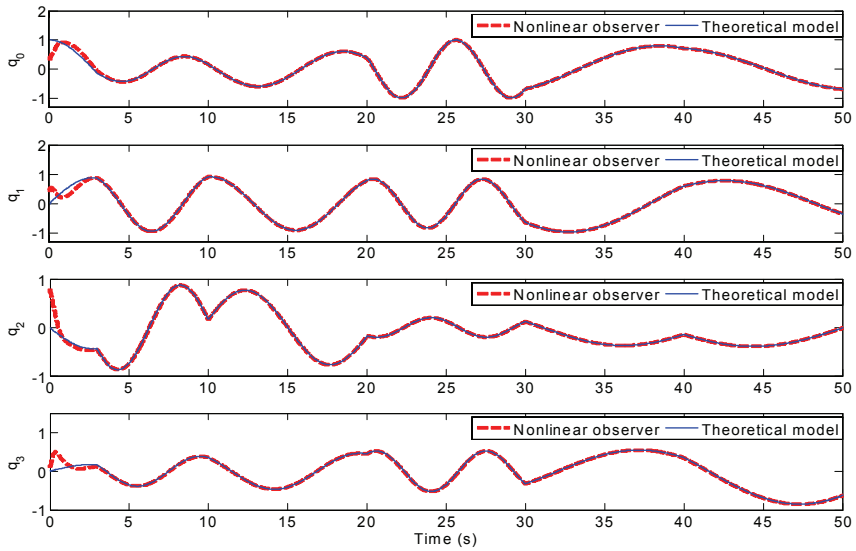

Fig. 3. Theoretical quaternion q and its estimated values $\hat{q}$

Table 1. Characteristics of the various noises for the sensors' measurements

Sensors	Parameters	Standard deviations	Units
Accelerometer	δ_f	0.01	m/s^2
Magnetometer	δ_h	0.03	*Gauss*
Gyroscope	δ_G	0.01	rad/s

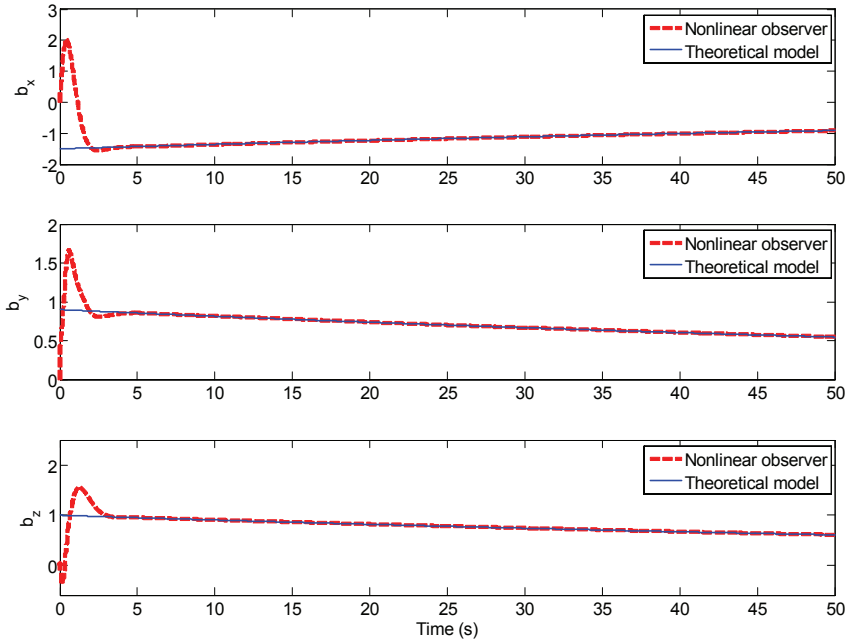

Fig. 4. Theoretical bias b and its estimation $\hat{b}$

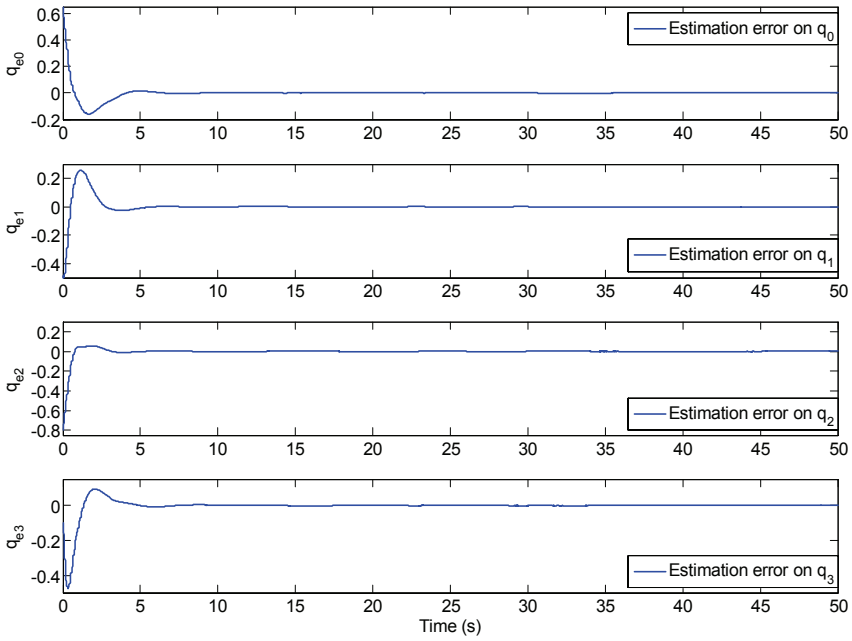

Fig. 5. Quaternion estimation errors

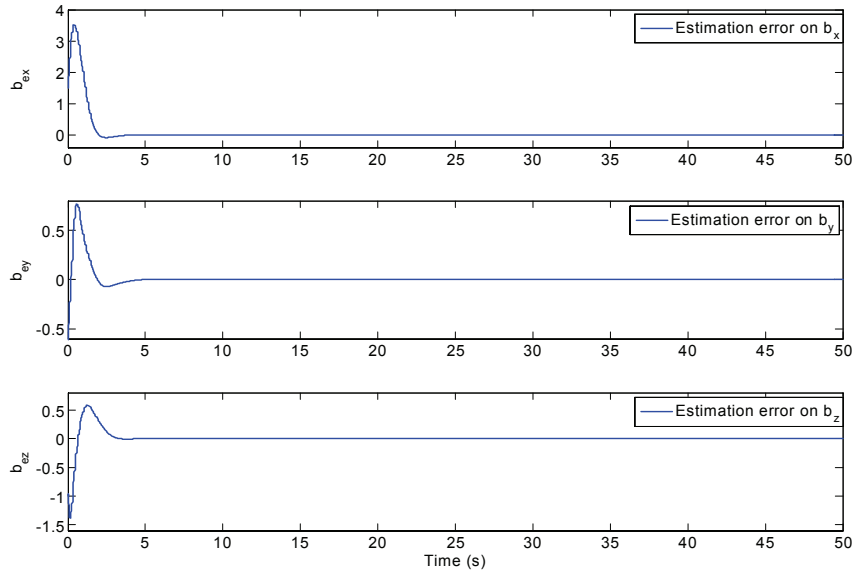

Fig. 6. Gyro-bias estimation errors

Table 2. Initial conditions

	Quaternion	Bias
Theoretical model	$q(t_0)=[1 \quad 0 \quad 0 \quad 0]^T$	$b(t_0)=[-1.5 \quad 0.9 \quad 1]^T$
Nonlinear observer	$\hat{q}(t_0)=[0.3 \quad 0.5 \quad 0.8 \quad 0.1]^T$	$\hat{b}(t_0)=[0 \quad 0 \quad 0]^T$

7. Experimental results

In order to evaluate the efficiency of the proposed approach in real word applications, an experimental setup was developed resorting to an inertial and magnetic sensor module. In this study, an Inertial Measurement Units (IMU) was employed: the MTi from Xsens Technologies [25], which outputs data at a rate of 100Hz. This MEMS device is a miniature, light weight, 3D digital output sensor (it outputs 3D acceleration (from accelerometer), 3D angular rate (from gyroscope), and 3D magnetic field data (from magnetometer)) with built-in bias, sensitivity, and temperature compensation. In the set of experiments, the calibrated data from MTi are used as inputs to the proposed nonlinear observer. In addition, this device is designed to track the body 3-D attitude output in Euler angles, quaternion or rotation matrix representations. The attitude from MTi is computed using an internal algorithm based on Xsens Kalman Filter (XKF) [25]. Note that MTi serves as tools for evaluation of the efficiency of the proposed attitude estimation algorithm.

In this paper, we choose to start our preliminary experiments by a simple motion in space with the MTi to validate the proposed approach. Those on king penguin will be made when the developed algorithm is implemented on the designed embedded prototype. The experiments were realized as follow: the MTi is posed on the ground without any motion for few moments. After that we take the MTi and we make it undergo a motion in all directions. Finally we return back to the static position on the ground. During this experiment, the MTi records inertial and magnetic measurements and the 3D-orientation as a quaternion, and transmits these readings to a PC via USB port. After that, the calibrated data are used to generate the estimated attitude using the proposed nonlinear observer in (21). Figure 7 illustrates the calculated attitude, in quaternion term, by the MTi and the estimated one obtained by the nonlinear observer. This figure contains also the corresponding estimation error on each quaternion component. Notice that the convergence rate is very fast and the mismatch is always small. This figure illustrates the efficiency of the proposed approach to estimate the attitude of the MTi during the motion.

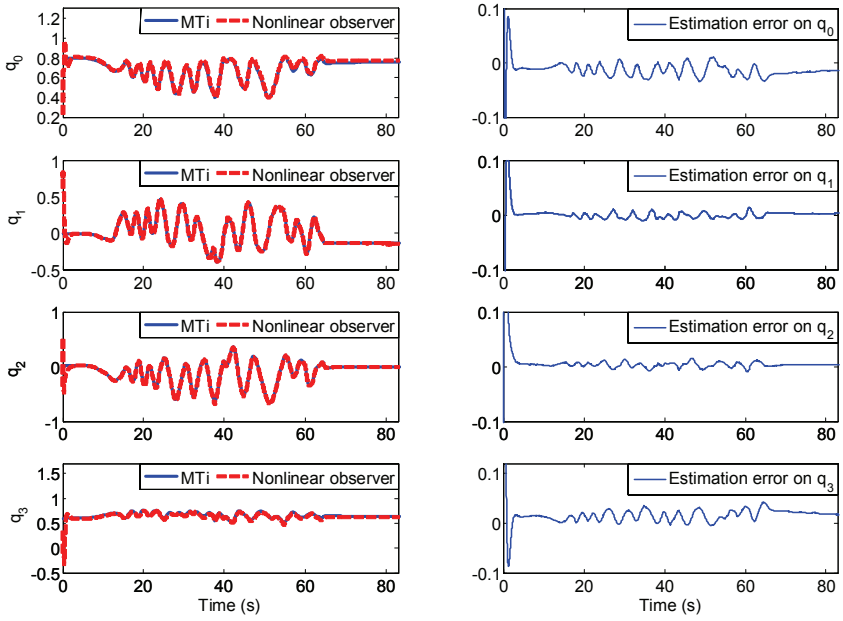

Fig. 7. Experimental and estimated attitude – the corresponding estimation errors

8. Conclusion and future work

An approach based on complementary nonlinear observer algorithm has been proposed to estimate the attitude (orientation) in order to improve the quality of measures obtained by using low-cost sensors. The goal of this work, dedicated to Bio-logging area, is to produce an animal posture tracking over wide motion range. The algorithm was developed based on the rigid-body kinematic equation. A quaternion-

based process model is built to avoid the problem of singularities as in Euler angle representations. The observer exploits the complementary aspect of measurements given by the attitude sensors (3-axis accelerometer and 3-axis magnetometer) and 3-axis gyroscope. The proposed approach combines a strap-down system, based on the integral of the angular velocity, with a Levenberg Marquardt Algorithm (LMA) that uses Earth's magnetic field and gravity vector to calculate attitude measurements. Moreover, this algorithm includes the estimation of rate gyros biases to compensate angular velocity measurements. The efficiency of the proposed approach has been shown from a set of numerical simulations and some experimental results. The first prototype, dedicated to this animal application, will be logged in future works on some animals (dog and horse) for preliminary tests.

References

1. Singh, S. P. N., Waldron, K. J.: Attitude estimation for dynamic legged locomotion using range and inertial sensors. IEEE International Conference on Robotics and Automation, Barcelona, Spain, (April 2005) 1663-1668.
2. Mahony, R., Hamel, T., Pflimlin, J. M.: Nonlinear complementary filters on the special orthogonal group. IEEE Transactions on Automatic Control, 53 (5) (2008) 1203-1218.
3. Sabatini, A. M.: Quaternion-based Extended Kalman Filter for determining orientation by inertial and magnetic sensing. IEEE Transactions on Biomedical Engineering, 53 (7) (2006) 1346-1356.
4. Boyd, I.L., Kato, A., Ropert-Coudert, Y.: Bio-logging science: sensing beyond the boundaries. Memoirs of the National Institute of Polar Research, 58 (2004) 1-14.
5. Halsey, L. G., Handrich, Y., Fahlman, A., Schmidt, A., Bost, C. A., Holder, R. L., Woakes, A. J., Butler, P. J.: Fine-scale analyses of diving energetics in king penguins Aptenodytes patagonicus: how behaviour affect costs of a foraging dive. Marine Ecology Progress Series, (344) (2007).
6. Elkaim, G.H., Decker, E.B., Oliver, G., Wright, B.: Marine Mammal Marker (MAMMARK) dead reckoning sensor for In-Situ environmental monitoring. IEEE Position, Loc. and Navigation Symposium, Monterey, USA, (April 2006) 976-987.
7. Johnson, M. P., Tyack, P. L.: A digital acoustic recording tag for measuring the response of wild marine mammals to sound. IEEE Journal of Oceanic Engineering, 28 (1) (2003) 3-12.
8. Watanabe, S., Isawa, M., Kato, A., Coudert, Y., Naito, Y.: A new technique for monitoring the behaviour of terrestrial animals; a case study with the domestic cat. Applied Animal Behaviour Science 94 (2005) 117-131.
9. Fourati, H., Afilal, L., Manamanni, N., Handrich, Y.: Data fusion solution for orientation of a slow-moving rigid body: Bio-logging application. 9th International Conference on Sciences and Techniques of Automatic Control & Computer Engineering, Sousse, Tunisia, (December 2008).
10. Bost, C. A., Handrich, Y., Butler, P. J., Fahlman, A., Halsey. G., Woakes, A. J., Coudert, Y.: Change in dive profiles as an indicator of feeding success in king and Adelie penguins. Deep-Sea Research II 54 (3-4) (2007) 248-255.
11. Wilson, R. P., Shepard, E. L. C., Liebsch, N.: Prying into the intimate details of animal lives: use of a daily diary on animals. Endangered Species Research, 4 (December 2007) 123-137.

12. Grewal, M. S., Weill, L. R., Andrews, A. P.: Global positioning systems, inertial navigation, and integration, John Wiley & Sons, Inc., (2001).
13. Kuipers, J.B.: Quaternion and Rotation Sequences. Princeton, NJ: Princeton University Press, (1999).
14. Shuster, M.D.: A survey of attitude representations. Journal Of the Astronautical Science, 41 (4) (1993) 493–517.
15. Beeby, S., Ensell, G., Kraft, M., White, N.: MEMS Mechanical Sensors, Artech House House Publishers, (2004).
16. Astrosurf, July 2009. Available: http://www.astrosurf.com/luxorion/terre-champ-magnetique2.htm.
17. Brown, R.G., Hwang, P.Y.C.: Introduction to Random Signal and Applied Kalman Filtering, 3rd Ed. New York: John Wiley, (1997).
18. Fourati, H., Manamanni, N., Afilal, L., Handrich, Y.: Rigid body motions estimation using inertial sensors: Bio-logging application. 7th IFAC Symposium on Modelling and Control in Biomedical Systems (including Biological Systems), Alborg, Danemark, (August 2009).
19. Salcudean, S.: A globally convergent angular velocity observer for rigid body motion. IEEE Transactions on Automatic Control, 36 (12) (1991) 1493-1497.
20. Khalil, H.: Nonlinear Systems, 3rd ed. NJ: Prentice-Hall, (2002).
21. Wahba, G.: A least squares estimate of spacecraft attitude. SIAM, Review, 7 (3) (1965) 409.
22. Dennis, J. E., Schnabel, R. B.: Numerical methods for unconstrained optimization and nonlinear equations. Prentice Hall, Englewood, NJ, (1983).
23. Fourati, H., Manamanni, N., Afilal, L., Handrich, Y.: A rigid body attitude estimation for Bio-logging application: A quaternion-based nonlinear filter approach. IEEE/RSJ International conference on intelligent robots and systems IROS'09, St. Louis, USA, (October 2009), 558-563.
24. Fourati, H., Manamanni, N., Afilal, L., Handrich, Y.: Nonlinear attitude estimation based on fusion of inertial and magnetic sensors: Bio-logging application. 2nd IFAC International Conference on intelligent Control Systems and Signal Processing, Istanbul, Turkey, (September 2009).
25. Xsens Technologies, Available: http://www.xsens.com (December 2009).